

# Supplementary Materials: Magnetic Nanoparticles with Dual Surface Functions – Efficient Carriers for Metalloporphyrin-Catalyzed Drug Metabolite Synthesis in Batch and Continuous-Flow Reactors

Diána Balogh-Weiser <sup>1,2,\*</sup>, Balázs Decsi <sup>1</sup>, Réka Krammer <sup>1</sup>, Gergő Dargó <sup>3</sup>, Ferenc Ender <sup>4,5</sup>, János Mizsei <sup>4</sup>, Róbert Berkecz <sup>6</sup>, Benjámín Gyarmati <sup>2</sup>, András Szilágyi <sup>2</sup>, Róbert Tóth <sup>7</sup>, Csaba Paizs <sup>7</sup>, László Poppe <sup>1,7</sup> and György T. Balogh <sup>3,8,\*</sup>

## 1. Characterization of Magnetic Carriers and Catalysts

### 1.1. Magnetic Separability of MNP-Catalysts in Batch Mode

A) suspension on MNP-Catalyst



B) magnetic separation



C) simultaneous separation by MagnaRack™ Magnetic Separation Rack

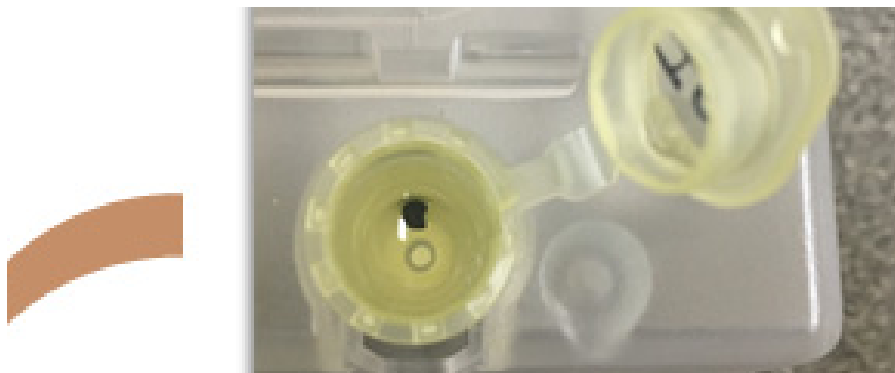


**Figure S1.** Illustration of magnetic separation of MNP-catalysts (surface grafted MNPs covered by metalloporphyrin FeTPFP or FeTPPS), stable suspension of MNP-catalyst **A**), magnetic separation of MNP-catalyst by permanent magnet **B**) and the parallel separation of MNP-catalysts by MagnaRack containing permanent magnets **C**). The MNP-catalysts were used in biomimetic oxidation of Amlodipine (**1**) in batch mode.

### 1.2. Magnetic Separability of MNP-Catalysts in Continuous-Flow Mode

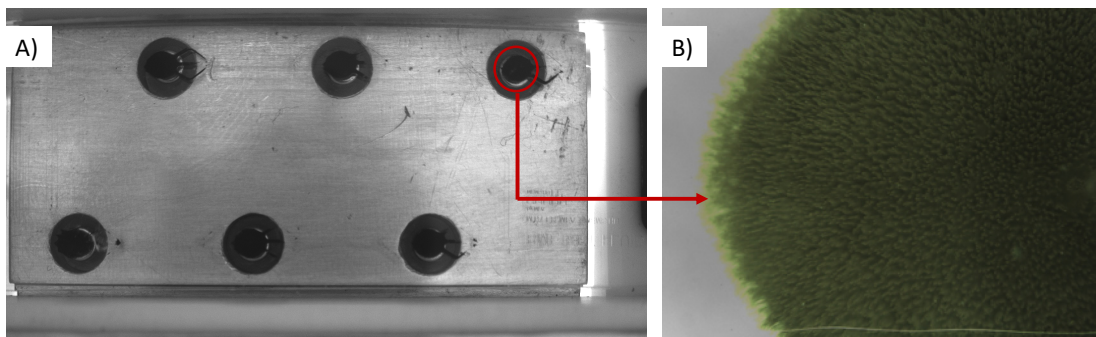


**Figure S2.** Photo of MNP-catalysts filled chip of continuous-flow Magnetic Chip reactor prepared by high speed USB camera **A)** and digital microscopic image of MNP-catalyst filled chamber **B)**.

### 1.3. Results of DLS Measurement of Magnetic Particles at Different Stages of Modifications

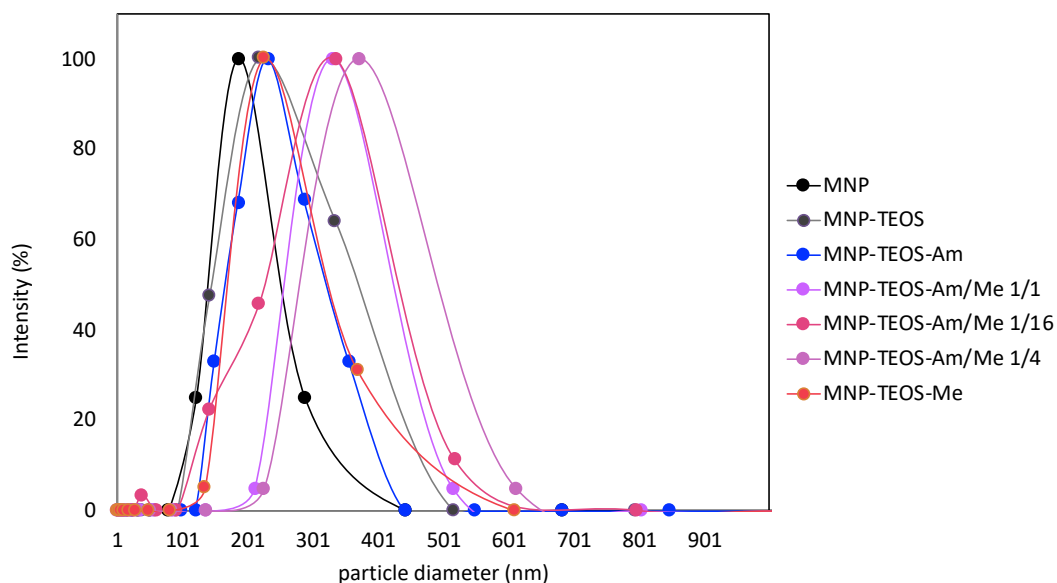


**Figure S3.** Determination of particle size distribution of magnetic particles at different stages of modification by DLS: MNP (naked magnetic particles), MNP-TEOS (MNP coated by silica layer by TEOS), MNP-TEOS-Am (MNP-TEOS surface grafted by pure amino-functions), MNP-TEOS-Am/Me 1/1 (MNP-TEOS surface grafted by amino- and methyl-functions at molar ratio 1/1), MNP-TEOS-Am/Me 1/4 (MNP-TEOS surface grafted by amino- and methyl-functions at molar ratio 1/4), MNP-TEOS-Am/Me 1/16 (MNP-TEOS surface grafted by amino- and methyl-functions at molar ratio 1/16), MNP-TEOS-Me (MNP-TEOS surface grafted by pure methyl-functions).

## 2. Results of HPLC-DAD-MS Analysis for Biomimetic Oxidation of Amlodipine (1)

### 2.1. HPLC-DAD Chromatograms of the Biomimetic Reactions

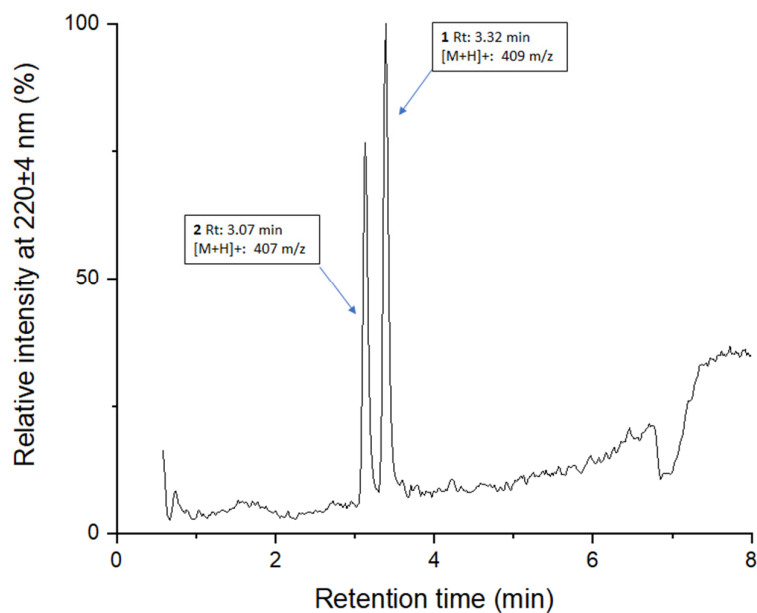


**Figure S4.** Representative HPLC data of FeTPFP-MNPs-catalyzed biomimetic oxidation of amlodipine (**1**) to major in vivo didehydro metabolite (**2**) in batch mode.

## 2.2. Identification of Amlodipine and its Metabolites by Mass Spectroscopy (MS)

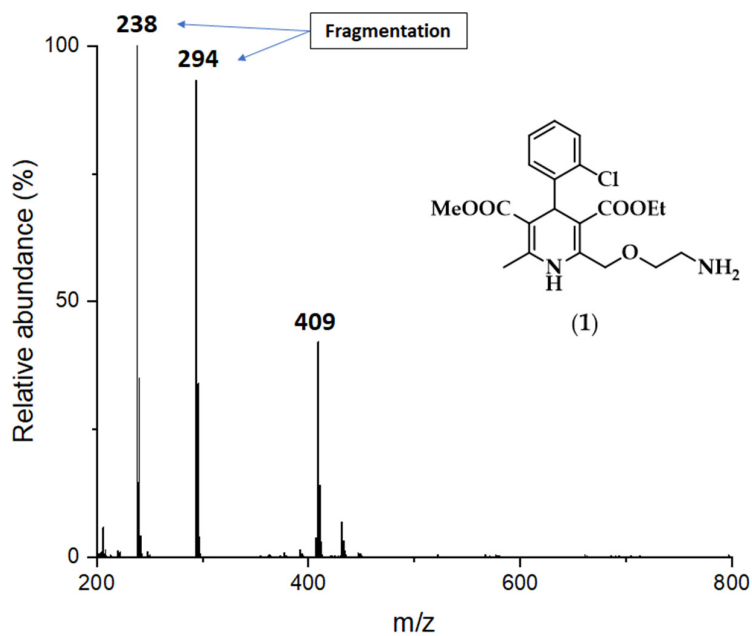


**Figure S5.** MS spectrum of amlodipine (**1**).

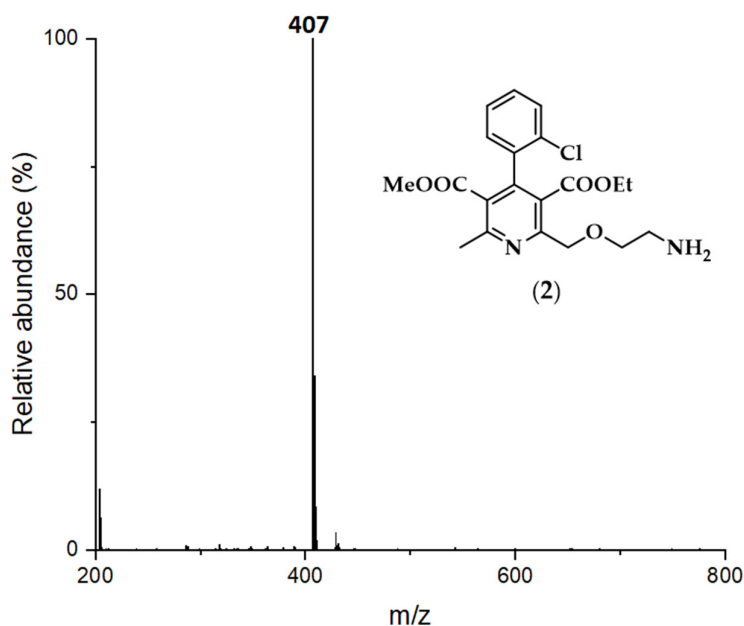


**Figure S6.** MS spectrum of amlodipine didehydro metabolite (2) as a main product of biomimetic oxidation.

### 3. Structural Identification of Amlodipine (1) and Amlodipine Metabolite (2) via HRMS Fragmentation and NMR.

#### 3.1. Summary of Retention Time, Observed Parent- and Characteristic Fragment Ions of Amlodipine and Didehydro Amlodipine

**Table S1.** Summary of retention time, observed parent- and characteristic fragment ions of amlodipine and didehydro amlodipine.

Compound	RT (min)	[M+H] <sup>+</sup> (m/z)	Mass error (ppm)	Collision Energy (eV)	Fragment ions (m/z)
Amlodipine	3.59	409.15276	0.69	20	377.12673, 294.08986, 238.06332 <sup>1</sup> 390.11102, 364.09539,
Dehydro-amlodipine	3.22	407.13747	0.84	25	364.08483, 318.05351, 286.02732 <sup>1</sup>

<sup>1</sup> most abundant fragment ion.

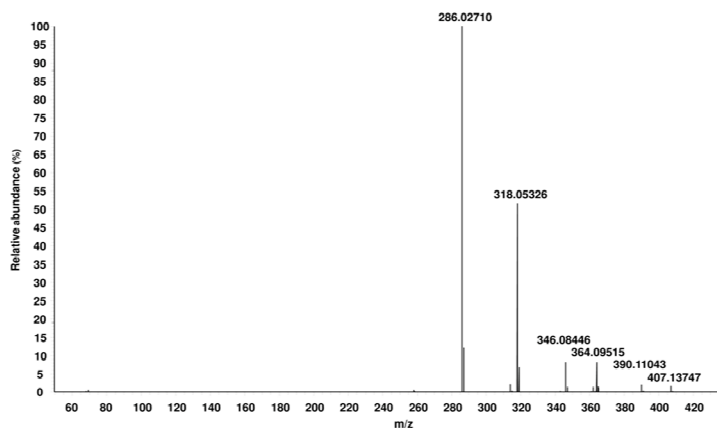


**Figure S7.** HRMS\MS spectrum of amlodipine didehydro metabolite (2) as a main product of biomimetic oxidation.

### 3.2. NMR Spectra of Didehydro Amlodipine Metabolite (2)

$^1\text{H}$  NMR (500 MHz,  $\text{CD}_3\text{-OD}$ ,  $\delta$  ppm): 7.79-7.87 (2H, m, H-34, 33), 7.48 (1H, dd,  $J = 8$  Hz,  $J = 1.3$  Hz, H-21), 7.40 – 7.45 (4H, m, H-32, 31, 30, 19), 7.36 (1H, td,  $J = 7.5$  Hz,  $J = 1.4$  Hz, H-17), 7.18 (1H, dd,  $J = 7.6$  Hz,  $J = 1.6$  Hz, H-18), 4.80 – 4.84 (2H, m, H-9), 3.96 – 4.05 (2H, m, H-2), 3.70 (2H, t,  $J = 5.2$  Hz, H-7), 3.53 (3H, s, H-10) 3.04 – 3.10 (2H, m, H-6) 2.63 (3H, s, H-15), 1.90 (56H, s, H39), 0.91 (2H, t,  $J = 7.2$  Hz, H-1) ppm.

$^{13}\text{C}$  NMR (126 MHz,  $\text{CD}_3\text{-OD}$ ,  $\delta$  ppm): 180.3 (C-40) 168.5 (C-13), 167.9 (C-14), 157.8 (C-28), 157.0 (C-24), 46.8 (C-25), 146.4 (C-35), 136.1 (C-20), 134.1 (C-22), 131.8 (C-18), 131.7 (C-30), 131.5 (C-31, 32), 130.5 (C-21), 130.3 (C-27) 129.4 (C-19), 128.3 (C-19), 128.1 (C-23), 127.7 (C-17), 127.1 (C-34, 33), 73.5 (C-9), 69.0 (C-7), 63.0 (C-2), 53.0 (C-10), 40.9 (C-6), 24.2 (C-39), 23.1 (C-15), 14.0 (C-1)